

# Kinetics and Inhibition of Reductive Dechlorination of Trichloroethene, *cis*-1,2-Dichloroethene and Vinyl Chloride in a Continuously Fed Anaerobic Biofilm Reactor

Sudeep C. Popat<sup>†,‡,§</sup> and Marc A. Deshusses<sup>‡,\*</sup>

<sup>†</sup>Department of Chemical and Environmental Engineering, University of California, Riverside, California 92521, United States

<sup>‡</sup>Department of Civil and Environmental Engineering, Duke University, Durham, North Carolina 27708, United States

<sup>§</sup> Supporting Information

**ABSTRACT:** Anaerobic bioreactors containing *Dehalococcoides* spp. can be effective for the treatment of trichloroethene (TCE) contamination. However, reductive dehalogenation of TCE often results in partial conversion to harmless ethene, and significant production of undesired *cis*-1,2-dichloroethene (*cis*-DCE) and vinyl chloride (VC) is frequently observed. Here, a detailed modeling study was conducted focusing on the determination of biokinetic constants for the dechlorination of TCE and its reductive dechlorination intermediates *cis*-DCE and VC as well as any biokinetic inhibition that may exist between these compounds. Dechlorination data from an anaerobic biotrickling filter containing *Dehalococcoides* spp. fed with single compounds (TCE, *cis*-DCE, or VC) were fitted to the model to determine biokinetic constants. Experiments with multiple compounds were used to determine inhibition between the compounds. It was found that the Michaelis–Menten half-saturation constants for all compounds were higher than for cells grown in suspended cultures, indicating a lower enzyme affinity in biofilm cells. It was also observed that TCE competitively inhibited the dechlorination of *cis*-DCE and had a mild detrimental effect on the dechlorination of VC. Thus, careful selection of biotreatment conditions, possibly with the help of a model such as the one presented herein, is required to minimize the production of partially dechlorinated intermediates.

## INTRODUCTION

Trichloroethene (TCE) is a persistent soil and groundwater pollutant that is known to cause several human health hazards.<sup>1,2</sup> Recently, a novel approach to biologically remediate sites contaminated with TCE was described.<sup>3</sup> The vision is to conduct soil vapor extraction or dual-phase extraction with nitrogen gas sparging and combine this with anaerobic biological treatment of TCE-laden waste gas streams thus generated. A lab-scale prototype anaerobic biotrickling filter was developed and exhibited excellent elimination capacities for TCE.<sup>3</sup> The biotrickling filter was inoculated with a mixed culture containing *Dehalococcoides* spp. These *Dehalococcoides* spp. expressed two reductive dehalogenases necessary for complete reduction of TCE to nontoxic ethene via *cis*-1,2-dichloroethene (*cis*-DCE) and vinyl chloride (VC): TceA, which is responsible for conversion of TCE and *cis*-DCE to VC, and VcrA, which is responsible for conversion of TCE, *cis*-DCE, and VC to ethene. Hydrogen necessary for dechlorination by these novel microorganisms was generated by fermentation of lactate, which was the substrate fed through the recirculating liquid.

Despite the high rates of TCE removal achieved, incomplete conversion to ethene was observed under all conditions. The accumulation of *cis*-DCE and VC in the exit gas stream is in contrast with batch cultures containing *Dehalococcoides* spp. that almost always result in complete conversion of TCE to ethene over time, with only transient production of the intermediates.<sup>4–7</sup> Preliminary batch studies with the biotrickling filter showed higher rates of *cis*-DCE and VC reduction than during continuous

operation,<sup>3</sup> suggesting that competitive inhibition between the various compounds may exist during continuous operation.

Chung et al.<sup>8</sup> observed a similar phenomenon with their continuously fed membrane biofilm reactor treating TCE-contaminated water. Despite the presence of the relevant reductive dehalogenases (BvcA in this case, instead of VcrA), it took over 100 days to reach appreciable conversion of TCE to ethene with significant accumulation of *cis*-DCE and VC in the outlet liquid stream. Azizian et al.<sup>9</sup> also observed significant accumulation of *cis*-DCE and VC in the outlet stream of a continuous flow column fed with perchloroethene (PCE)-contaminated water. Although conversion to ethene was improved with increasing lactate load, competitive inhibition may have resulted in the accumulation of intermediates. Even in situ bioremediation applications, there are reports of incomplete dechlorination despite the presence of *Dehalococcoides* spp. Most notably, the Naval Weapons Station site in Seal Beach, CA, which was bioaugmented with KB-1 culture, had persisting *cis*-DCE even after two months of bioaugmentation.<sup>10</sup> Eventually, the site was completely remediated,<sup>11</sup> but the persistence of *cis*-DCE for a significant duration may have been a direct result of biokinetic competition, as long as PCE and TCE were not entirely dechlorinated.

**Received:** August 19, 2010

**Accepted:** December 7, 2010

**Revised:** December 3, 2010

**Published:** January 11, 2011

Various researchers have evaluated the kinetics and inhibition of reductive dechlorination of chlorinated ethenes using batch-fed suspended cultures.<sup>12–16</sup> Even so, there is no consensus on which compounds inhibit the dechlorination of which compounds. Also, there are no reports on the kinetics and inhibition of reductive dechlorination of chlorinated ethenes by cultures that are immobilized, and only one report on a continuously fed system,<sup>17</sup> although the aims of the study were to evaluate toxicity at high concentrations of chlorinated ethenes and not biokinetic inhibitions between the various compounds.

Reported here is a detailed study on the determination of biokinetic constants and inhibition of reductive dechlorination of TCE, *cis*-DCE, and VC by a *Dehalococcoides* spp.-containing biofilm in an anaerobic biotrickling filter continuously treating TCE vapors. A detailed model that accurately describes all relevant transport and biological phenomena in the biotrickling filter was developed. Experiments on the dechlorination of TCE, *cis*-DCE, and VC either alone or in mixtures in the biotrickling filter operated in a differential mode were used to obtain biokinetic constants and used for model validation.

## MATERIALS AND METHODS

**Biotrickling Filter Setup and Differential Operation.** The continuous biotrickling filter treating TCE vapors used in this study was identical to the setup described by Popat and Deshusses,<sup>3</sup> except that the bed height was slightly smaller (28 cm bed height and 10 cm ID) resulting in a total bed volume of 2.2 L, the liquid sump volume was reduced to 500 mL, and a liquid recirculation rate of 60 mL min<sup>-1</sup> was used. The packing material used was cattle bone Porcelite (CBP, Aisin Takaoka Co., Ltd., Japan), a microporous ceramic.<sup>18</sup> The bed porosity was determined to be 42% by measuring the volume of water needed to fill the voids in a given bed volume. The biotrickling filter was initially inoculated with SDC-9, a commercially available mixed culture containing *Dehalococcoides* spp. (SDC-9, Shaw Environmental, Inc., Lawrenceville, NJ); see the Supporting Information of ref 3 for details on the culture.

For experiments with the differential biotrickling filter, the reactor was operated in batch mode with respect to both the gas and liquid streams (Figure S1 of the Supporting Information). The gas inlet and outlet ports of the reactor were connected to both ends of a custom-made 25 L gas Tedlar bag (SKC Inc., Eighty Four, PA) serving as a gas reservoir. The liquid trickling rate was kept unchanged during batch operation, but the fresh liquid feed was discontinued. A gas diaphragm pump (Gast Manufacturing, Inc., Benton Harbor, MI) was connected between the Tedlar bag and the reactor to recirculate the gas in a closed loop at a high velocity. A gas flow rate of 0.94 m<sup>3</sup> h<sup>-1</sup> was achieved using the diaphragm pump. Such high gas velocity allowed operating the biotrickling filter without any transport limitation in the gas film and with minimum axial gradients. During continuous operation, the reactor was operated in concurrent mode with respect to the gas and liquid, and during differential operation, the gas entered from the bottom of the bed, while the liquid was trickled from the top.

Sodium lactate (3–5 g L<sup>-1</sup>, Alfa Aesar, Ward Hill, MA) was provided to the biotrickling filter via the recirculating liquid. Lactate was at least 10 times in excess of the stoichiometric requirement for production of hydrogen necessary for complete dechlorination. Methane generation was used as an indication of hydrogen availability or absence of electron donor limitation

because SDC-9 contains only hydrogenotrophic methanogens. The rate of methane formation remained relatively constant during all experiments, and dechlorination was not a function of the excess lactate if supplied at greater than 5 fold excess. Together, this indicates that there was no hydrogen limitation during these experiments. Fresh mineral medium (see Popat and Deshusses<sup>3</sup> for composition) was used for each experiment. The pH of the fresh medium was always adjusted to between 7.0 and 7.2.

All the experiments with the differential biotrickling filter were carried out after a steady state was reached in continuous operation (3 months after initial bioreactor start-up). The TCE elimination capacity for the biotrickling filter during continuous operation remained around 2 g m<sub>bed</sub><sup>-3</sup> h<sup>-1</sup> at an empty bed residence time (EBRT) of 3 min during the entire study, with >50% conversion of the removed TCE to *cis*-DCE and <20% conversion to ethene. This is in the same range as observed in our previous studies.<sup>3</sup>

**Modeling Analyses.** Each experiment for curve fitting, parameter validation, or determination of inhibitions began with cleaning the entire system by flushing with nitrogen gas for at least 1 h, during which the outlet gas concentrations were measured. Once no chlorinated species could be detected in the outlet gas stream, a Tedlar bag with a known concentration of TCE, *cis*-DCE, VC, or mixture of any two compounds was connected to the biotrickling filter along with the diaphragm pump. The experimental protocol included measuring the concentrations of each compound, as well as methane, in the Tedlar bag at regular intervals for the duration of the experiments, which was usually 4 h. Experiments with single compounds were conducted with three different concentrations. One data set was used for curve fitting to determine  $R_{\max}$  and  $K_m$  values, while the other two data sets were compared to the model predictions using the estimated kinetic constants and served as validation. The best set of  $R_{\max}$  and  $K_m$  values for the data set used in curve fitting was determined using the least-squares analysis method that minimizes the sum of the squared residuals. For determining inhibitions between various compounds, mixtures of TCE, *cis*-DCE, and VC were treated. In general, two compounds were treated together with one fixed concentration for one compound and both absence of and two different concentrations of the other compound. Experimental data were compared with model simulations considering either competitive inhibition or absence of inhibition. The sum of the squared residuals was used as criterion to decide which prediction was best.

**Analytical Techniques.** Gas-phase concentrations of TCE, *cis*-DCE, VC, ethene, and methane were determined using an HP 5890 gas chromatograph fitted with a 30 m GS-Q column (0.32 mm ID, Agilent Technologies Inc., Wilmington, DE) and a flame ionization detector. A gas sampling valve and a 5 mL loop was used for automated injection into the GC. The detection limits for the compounds in gas samples were: 0.002 g m<sup>-3</sup> for TCE, 0.001 g m<sup>-3</sup> for *cis*-DCE and VC, and 0.0005 g m<sup>-3</sup> for ethene and methane. The TOC content of the recirculating liquid was determined using a Shimadzu TOC-5050 analyzer (Shimadzu Scientific Instruments, Columbia, MD), while DO concentration, ORP, and pH were determined using Vernier probes and data loggers (Vernier Software & Technology, Beaverton, OR).

The protein content of packing samples taken from the biotrickling filter bed was determined at the end of the study as follows. Packing material was taken from different heights of the bed, and biomass was lightly scraped off into sterile deionized water. The solution was then flowed through a preweighed 0.45 μm pore filter. The filter was vacuum-dried for 24 h at

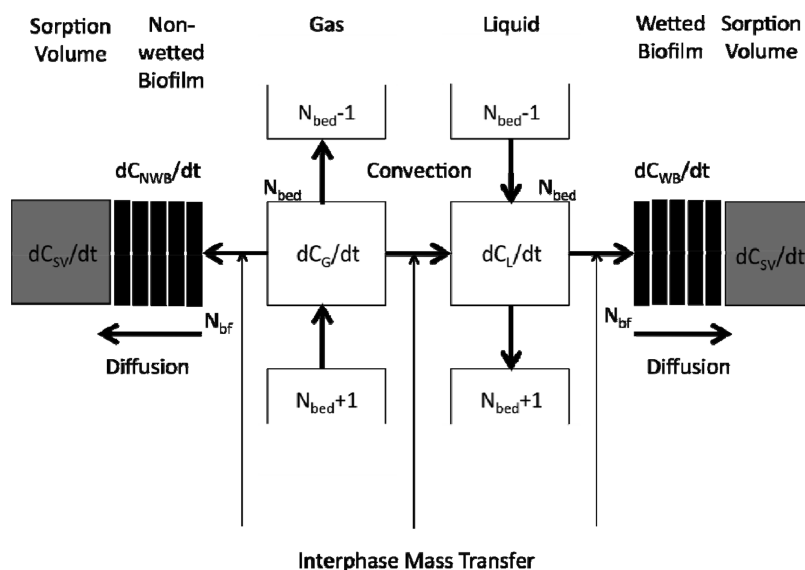


Figure 1. Schematic of the model structure showing one finite (horizontal layer) in the biotrickling filter.

60 °C, and reweighed to determine the dry biomass content. Protein content was assumed to be 60% of the dry biomass weight.

## MODEL DEVELOPMENT

**Model Concept and Assumptions.** To accurately determine the real biokinetic constants for reductive dechlorination of TCE, *cis*-DCE, and VC, and to elucidate various inhibitions, a model that attempts to make an exact representation of transport and biokinetic processes occurring in the anaerobic biotrickling filter was developed. A schematic of the model concept is shown in Figure 1. The model considers four different active phases: gas, liquid, biofilm, and sorption volume within the pores of the packing material. For finite differences, the bed is divided into a number of vertical segments, while the biofilm is divided into a number of horizontal segments.

The following assumptions were made to develop the model equations:

1. Throughout the height of the bed, the thickness of the biofilm is uniform.
2. Each segment as defined in Figure 1 and the Tedlar bag gas reservoir are completely mixed.
3. The biofilm is not completely wetted. Liquid trickling velocities used in biotrickling filters are low, and thus, there are sections of biofilm that do not have a continuously flowing liquid film on top.<sup>19</sup> In such a case, compounds of interest, apart from transferring from the gas to the biofilm via the liquid, can also transfer directly from the gas to the biofilm. Additionally, it was considered that there are no dynamic changes in wetting.
4. Because the packing material contains a large number of micropores, there is a certain static liquid hold-up inside the matrix that can absorb compounds from the biofilm. It was, however, assumed that no active cells are present in these micropores.<sup>20</sup>
5. Gas flow throughout the bed height is by plug flow, as high gas velocities result in large Peclet numbers (>10). Thus, there is also no radial heterogeneities or axial dispersion.
6. Convective mass transfer rates between different phases are expressed using mass transfer coefficients determined

from empirical equations available in the literature. Additionally, mass transfer coefficients for the gas side for transfer to both liquid and biofilm are the same. Diffusion within the biofilm is described by Fick's law.

7. Kinetics of reductive dechlorination of TCE and its intermediates are described by Michaelis–Menten enzyme kinetics. Possible competitive inhibition exists between the different chlorinated ethenes, but the daughter products do not inhibit the reductive dechlorination of the parent compounds. This assumption was based on the previous results of Yu et al.<sup>15</sup> and Schaefer et al.,<sup>16</sup> however, independent verification was made in this study as described in the Results and Discussion section. All inhibition constants are assumed to be equal to the half-saturation constants of the same compound consistent with the hypothesis that each compound can bind to the active sites of the reductive dehalogenase enzymes. However, as described later, that was not the case in one specific inhibition (TCE on VC).
8. Reductive dechlorination is not limited by hydrogen availability. This implies that lactate fermentation is not rate-limiting. Fermentation reactions in general proceed at a much faster rate than reductive dechlorination. In addition, experience with similar reactors and various lactate feed rates above five times the stoichiometric requirement for complete reductive dechlorination showed very little effect on reductive dechlorination (data not shown). Methane concentrations in these cases increase with increase in lactate feed, and in the presence of primarily hydrogenotrophic methanogens, this indicates ample hydrogen availability.
9. There is no net increase in biomass over the entire experimental period, as all experiments were done after the biotrickling filter had reached a steady state and were short term. This was also qualitatively confirmed by periodically weighing the reactor, which showed no net increase over 2 months (data not shown). The fraction of the dechlorinating biomass also remains constant. Experiments with similar reactors showed that after the startup period, a steady number of copies of the genes encoding for the TceA and VcrA enzymes was achieved (in the order of  $10^7$  copies per g of packing, unpublished results).

10. There is no biological reaction in the trickling liquid phase.

This is a reasonable assumption because the amount of biomass present in the liquid is negligible. To independently confirm this, however, selected liquid samples were incubated from when the reactor was running continuously with lactate and TCE, *cis*-DCE, or VC under anaerobic conditions, and no appreciable reduction was observed over 6 h (data not shown).

11. The effect of pH is neglected. Over the course of any particular experiment, the pH of the recirculating liquid changed by no more than 0.2 units.

**Model Equations.** The model equations described below were derived from the above model structure and assumptions. All equations are described as finite mass balances over the active phases considered. Equations for each different compound are not repeated here; instead general equations are listed with the index *cmpd* standing for TCE, *cis*-DCE, VC, and ethene. The vertical bed segments are denoted by *i*, while the horizontal biofilm segments are denoted by *j*.

Gas phase:

$$V_G \frac{dC_{G, \text{cmpd}}[i]}{dt} = F_G (C_{G, \text{cmpd}}[i+1] - C_{G, \text{cmpd}}[i]) - k_G A_W (C_{G, \text{cmpd}}[i+1] - C_{GLi, \text{cmpd}}[i]) - k_G A_{NW} (C_{G, \text{cmpd}}[i] - C_{GBi, \text{cmpd}}[i]) \quad (\text{Equation 1})$$

Liquid phase:

$$V_L \frac{dC_{L, \text{cmpd}}[i]}{dt} = F_L (C_{L, \text{cmpd}}[i-1] - C_{L, \text{cmpd}}[i]) + k_G A_W (C_{G, \text{cmpd}}[i] - C_{GLi, \text{cmpd}}[i]) - k_L A_W (C_{L, \text{cmpd}}[i] - C_{LBi, \text{cmpd}}[i]) \quad (\text{Equation 2})$$

For the mass balance over the wetted and nonwetted biofilms, three different equations were needed: one for the first layer of biofilm in contact with the liquid or gas, one for the last layer of biofilm in contact with the sorption volume, and one for all the intermediate biofilm segments. The sum of rate of appearance and disappearance of any compound (TCE, *cis*-DCE, VC, and ethene) due to biological reaction is denoted by  $R_{\text{cmpd}}$  in the following equations and is developed later.

Wetted biofilm first layer:

$$\frac{dC_{WB, \text{cmpd}}[i, 1]}{dt} = \frac{k_L A_W}{V_{WB}} (C_{L, \text{cmpd}}[i] - C_{LBi, \text{cmpd}}[i]) - \frac{D_{e, \text{cmpd}}}{Z^2} (C_{WB, \text{cmpd}}[i, 1] - C_{WB, \text{cmpd}}[i, 2]) - R_{\text{cmpd}} \quad (\text{Equation 3})$$

Wetted biofilm intermediate layers:

$$\frac{dC_{WB, \text{cmpd}}[i, j]}{dt} = \frac{D_{e, \text{cmpd}}}{Z^2} (C_{WB, \text{cmpd}}[i, j-1] - 2C_{WB, \text{cmpd}}[i, j] + C_{WB, \text{cmpd}}[i, j+1]) - R_{\text{cmpd}} \quad (\text{Equation 4})$$

Wetted biofilm last layer:

$$\frac{dC_{WB, \text{cmpd}}[i, N]}{dt} = \frac{D_{e, \text{cmpd}}}{Z^2} (C_{WB, \text{cmpd}}[i, N-1] - 2C_{WB, \text{cmpd}}[i, N] + C_{SV, \text{cmpd}}[i]) - R_{\text{cmpd}} \quad (\text{Equation 5})$$

Nonwetted biofilm first layer:

$$\frac{dC_{NWB, \text{cmpd}}[i, 1]}{dt} = \frac{k_G A_{NW}}{V_{NWB}} (C_{G, \text{cmpd}}[i] - C_{GBi, \text{cmpd}}[i]) - \frac{D_{e, \text{cmpd}}}{Z^2} (C_{NWB, \text{cmpd}}[i, 1] - C_{NWB, \text{cmpd}}[i, 2]) - R_{\text{cmpd}} \quad (\text{Equation 6})$$

Nonwetted biofilm intermediate layers:

$$\frac{dC_{NWB, \text{cmpd}}[i, j]}{dt} = \frac{D_{e, \text{cmpd}}}{Z^2} (C_{NWB, \text{cmpd}}[i, j-1] - 2C_{NWB, \text{cmpd}}[i, j] + C_{NWB, \text{cmpd}}[i, j+1]) - R_{\text{cmpd}} \quad (\text{Equation 7})$$

Nonwetted biofilm last layer:

$$\frac{dC_{NWB, \text{cmpd}}[i, N]}{dt} = \frac{D_{e, \text{cmpd}}}{Z^2} (C_{NWB, \text{cmpd}}[i, N-1] - 2C_{NWB, \text{cmpd}}[i, N] + C_{SV, \text{cmpd}}[i]) - R_{\text{cmpd}} \quad (\text{Equation 8})$$

Sorption volume:

$$V_{SV} \frac{dC_{SV, \text{cmpd}}[i]}{dt} = \frac{D_{e, \text{cmpd}} A_W}{Z} (C_{WB, \text{cmpd}}[i, N] - C_{SV, \text{cmpd}}[i]) + \frac{D_{e, \text{cmpd}} A_{NW}}{Z} (C_{NWB, \text{cmpd}}[i, N] - C_{SV, \text{cmpd}}[i]) \quad (\text{Equation 9})$$

The rate of biological reaction,  $R_{\text{cmpd}}$  is described using Michael-Menten type kinetics as in Equation 10. This rate considers both appearance and disappearance of the compound (no appearance due to biological reaction in the case of TCE, and no disappearance due to biological reaction in the case of ethene), along with competitive inhibitions. The following reaction is written for the wetted biofilm; for nonwetted biofilm all concentrations should be replaced with those in the non-wetted biofilm.

$$R_{\text{cmpd}} = \frac{R_{\text{max, parent}} C_{WB, \text{parent}}}{K_{M, \text{parent}} \left( 1 + \frac{C_{WB, \text{inhib}}}{K_{M, \text{inhib}}} \right) + C_{WB, \text{parent}}} - \frac{R_{\text{max, cmpd}} C_{WB, \text{cmpd}}}{K_{M, \text{cmpd}} \left( 1 + \frac{C_{WB, \text{inhib}}}{K_{M, \text{inhib}}} \right) + C_{WB, \text{cmpd}}} \quad (\text{Equation 10})$$

**Model Parameters.** All model parameters fall in two broad categories: physicochemical properties of the compounds, and system specific mass transfer or kinetic constants. The primary objective of the study was to determine the real biokinetic constants using model fitting of experimental results and then to validate the model by predicting the outcome of other experiments. All the determined parameters are listed in Table 1.

Henry's law constants for each compound were from the literature.<sup>21</sup> The effective diffusivities of the compounds in biofilm were determined by first using the Wilke–Chang correlation<sup>22</sup> for determining the effective diffusivities in water and then by correcting those as 29% of the value for TCE, *cis*-DCE, and VC, and 43% of the value for ethene, as per Stewart.<sup>23</sup> The specific surface area of the biotrickling filter bed packing was

Table 1. List of Model Parameters apart from Kinetic Constants

parameter	value
Henry's law constant for TCE, $H_{TCE}$	0.392 (–)
Henry's law constant for <i>cis</i> -DCE, $H_{cis-DCE}$	0.167 (–)
Henry's law constant for VC, $H_{VC}$	1.137 (–)
Henry's law constant for ethene, $H_{ETH}$	8.567 (–)
effective diffusion coefficient for TCE in biofilm, $D_{e,TCE}$	$6.47 \times 10^{-7} \text{ m}^2 \text{ h}^{-1}$
effective diffusion coefficient for <i>cis</i> -DCE in biofilm, $D_{e,cis-DCE}$	$7.29 \times 10^{-7} \text{ m}^2 \text{ h}^{-1}$
effective diffusion coefficient for VC in biofilm, $D_{e,VC}$	$8.48 \times 10^{-7} \text{ m}^2 \text{ h}^{-1}$
effective diffusion coefficient for ethene in biofilm, $D_{e,ETH}$	$1.56 \times 10^{-6} \text{ m}^2 \text{ h}^{-1}$
specific surface area of biotrickling filter bed, $a$	$1160 \text{ m}^2 \text{ m}^{-3}$
fraction of total surface area that is wetted, $A_W/A_T$	49%
gas film mass transfer coefficient, $k_G$	$3.648 \text{ m h}^{-1}$
liquid film mass transfer coefficient, $k_L$	$0.022 \text{ m h}^{-1}$
total gas volume, $V_G$	30 L
liquid sump volume, $V_{sump}$	0.5 L
bed volume, $V_{bed}$	2.2 L
bed porosity, $\varepsilon$	42%
dynamic hold-up of the bed, $V_{DH}$	10%
sorption volume of bed (internal porosity of material), $V_{SV}$	50%
biofilm thickness, $Z$	18 $\mu\text{m}$
number of vertical bed segments, $N_{bed}$	5
number of horizontal biofilm segments, $N_{bf}$	5

determined as per Ottengraf.<sup>24</sup> The ratio of wetted area to total area was determined using the empirical equation proposed by Onda et al.<sup>25</sup> The gas- and liquid-film mass transfer coefficients were determined using empirical equations proposed by Kim and Deshusses<sup>26</sup> for the specific packing material used. The dynamic holdup of the bed was determined by stopping liquid recirculation and collecting and measuring the volume of the dripping liquid for 30 min. The sorption volume was determined from the internal porosity of the packing determined by Sakuma et al.<sup>18</sup> The biofilm thickness was determined gravimetrically at the end of the study for multiple samples of the packing material from various heights, assuming a homogeneous biofilm thickness around the spherical beads of packing. This was determined to be 18  $\mu\text{m}$ , which is very small compared to aerobic biotrickling filters.<sup>27</sup> Anaerobic microorganisms typically have a much lower biomass yield,<sup>28</sup> and this could be the reason for the thinner biofilm. The number of vertical bed segments and horizontal biofilm segments used for numerical simulations was five each as determined from the sensitivity of the model to these parameters.

## RESULTS AND DISCUSSION

**Determination of Biological Kinetic Constants.** To validate the assumption that no kinetic inhibition existed from daughter products on the dechlorination of parent compounds (Assumption 7), we conducted the following experiments. A *cis*-DCE reduction experiment was conducted in the presence of a higher concentration of VC, and a TCE reduction experiment was conducted in the presence of high concentrations of both *cis*-DCE and VC. No effect of the presence of the daughter products could be distinguished on the observed rate of reductive dechlorination of the parent compounds (Figures S2 and S3 of the Supporting Information), and thus the assumption was validated.

For both VC and *cis*-DCE only experiments, better curve fits were obtained for the products than for the parent compounds,

and thus these fits were used for biokinetic constants determination. In the case of VC, this was because of the use of VC stabilized in methanol, which resulted in conjoint peaks on the gas chromatograph for VC and methanol at the highest concentrations. In the case of *cis*-DCE, no definite reason was found for this behavior. As control, selected experiments were conducted with *cis*-DCE and TCE in the presence of methanol, and no effect of the presence of methanol on reductive dechlorination rates was observed (data not shown). This is consistent with the fact that all experiments were conducted with a large excess of electron donor, hence presence of a small amount of methanol had no effect.

In the next paragraphs, experimental results, model fitting for parameter determination, and model predictions are presented and discussed. Because biokinetic constants of the most dechlorinated compounds are needed to simulate the dechlorination of their parent compounds, experiments were conducted first with VC, then with *cis*-DCE, and finally with TCE. They are presented and discussed in this order. Figure 2 shows the comparison of the experimental data with model simulations for VC only experiments. A good fit was observed for the experimental data using the model, and the model predicted well the behavior of the system for the two other data sets.

Figure 3 shows the comparison of experimental data with model simulations for *cis*-DCE only experiments. Because VC concentration data was used for curve fitting, to accurately determine kinetic constants for *cis*-DCE, it was necessary to determine whether or not *cis*-DCE inhibited VC dechlorination. While this was studied in detail later, experimental data from *cis*-DCE experiments were fitted to two different models (one considering no inhibition of *cis*-DCE on VC dechlorination, and the other considering competitive inhibition of *cis*-DCE on VC dechlorination), and the model that resulted in the best curve fit, as well as better comparison with other data sets, was selected (data shown only for the best fit model). This turned out to be the model that had no inhibition of *cis*-DCE on VC dechlorination.

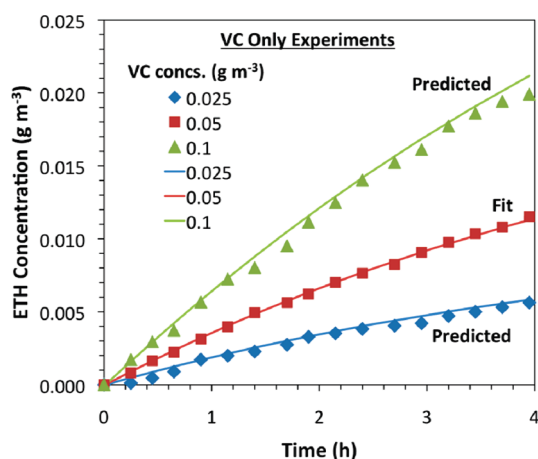


**Figure 2.** Comparison of experimental data (symbols) and model simulations (lines, either fitted or predicted) for VC only experiments. Legend shows initial concentrations of VC in  $\text{g m}^{-3}$ .

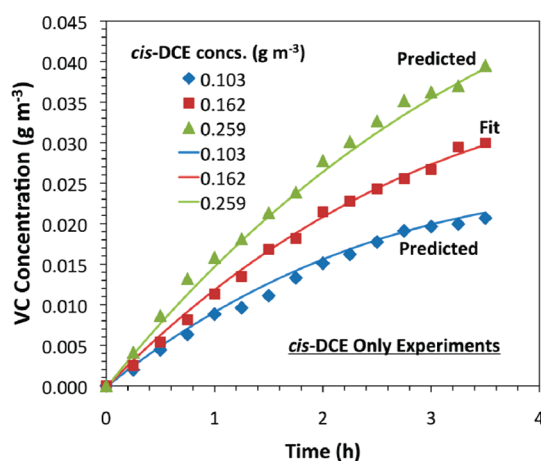


**Figure 3.** Comparison of experimental data (symbols) and model simulations (lines, either fitted or predicted) for *cis*-DCE only experiments. Legend shows initial concentrations of *cis*-DCE in  $\text{g m}^{-3}$ .

This, however, contradicts some results obtained by others with mixed cultures containing *Dehalococcoides* spp., where researchers found competitive inhibition of *cis*-DCE on VC dechlorination.<sup>15,16</sup> One of the reasons for this discrepancy could be that both *cis*-DCE and VC dechlorination were likely biocatalyzed in the present system by different enzymes (*cis*-DCE by the TceA enzyme, and VC by the VcrA enzyme), as discussed in detail later, whereas that may not have been the case in the other studies. The *cis*-DCE and ethene concentration data from *cis*-DCE only experiments were also compared to the model predictions using the estimated parameters for *cis*-DCE and VC and showed good agreement (Figures S4 and S5 of the Supporting Information).

Figure 4 shows the comparison of the experimental data with model fitted data ( $0.25 \text{ g m}^{-3}$ ) and model predictions ( $0.15$  and  $0.40 \text{ g m}^{-3}$ ) for TCE only experiments. The *cis*-DCE concentration data from TCE only experiments were also compared to model simulations using the estimated parameters for the two compounds as well as the inhibitions elucidated later in the study and showed good correlation (Figure S6 of the Supporting Information). The comparison of the VC and ethene concentration data set, however, did not show a good correlation for the two

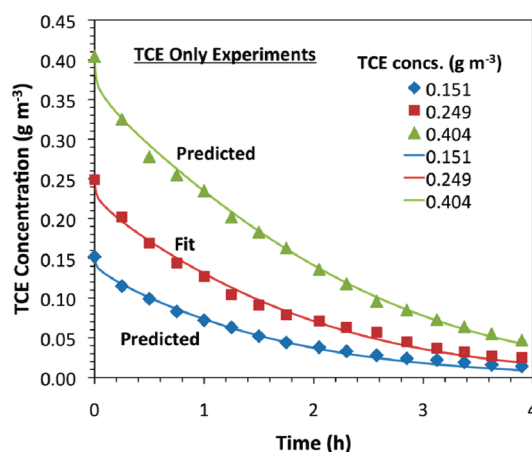


**Figure 4.** Comparison of experimental data (symbols) and model simulations (lines, either fitted or predicted) for TCE only experiments. Legend shows initial concentrations of TCE in  $\text{g m}^{-3}$ .

highest concentrations of TCE used (Figures S7 and S8 of the Supporting Information, which consider no inhibition of TCE on VC dechlorination). This could likely be because of the uncertainty in the inhibition of TCE on VC dechlorination as discussed later for Figure 7.

The  $R_{\text{max}}$  values for TCE, *cis*-DCE, and VC from the above fits were determined as 1381, 313, and  $706 \text{ mmol m}_{\text{biofilm}}^{-3} \text{ h}^{-1}$ , respectively. This indicates that *cis*-DCE dechlorination is the slowest of all three steps. In addition, the  $K_{\text{m}}$  value for *cis*-DCE was determined as  $6.9 \mu\text{M}$ , while those for TCE and VC were determined as  $5.3$  and  $4.1 \mu\text{M}$ , respectively, suggesting the poorest enzyme affinity for *cis*-DCE out of the three compounds. From a thermodynamic perspective, this is logical because the Gibbs free energy change resulting from coupling of *cis*-DCE reduction to hydrogen oxidation is the lowest in comparison to TCE or VC reduction.<sup>29</sup>

**Comparison with Other Studies with Batch Suspended Cultures.** A comparison with other studies with batch suspended cultures that have reported  $R_{\text{max}}$  and  $K_{\text{m}}$  values for the reductive dechlorination of TCE, *cis*-DCE, and VC is warranted. For this, the  $R_{\text{max}}$  values determined in this study were normalized to the total protein content of the biotrickling filter bed. Correction for some values in the table that are not reported on a per protein content basis was done using assumptions made by Schaefer et al.<sup>16</sup> The protein content in the present system was determined to be  $2750 \text{ mg}$ . As reported in Table 2, there is 3 orders of magnitude difference in the  $R_{\text{max}}$  values between those determined by us and by Schaefer et al.<sup>16</sup> using the same culture and 2 orders of magnitude difference between those determined by us and by Yu et al.<sup>15</sup> using two different cultures containing *Dehalococcoides* spp. One likely reason is the difference in the fraction of *Dehalococcoides* spp. cells present in the culture. In our reactor, significant hydrogenotrophic methanogenesis was continuously observed because the amount of lactate fed during continuous operation was at least 10 times the stoichiometric requirement for production of enough hydrogen for complete reductive dechlorination. This also probably resulted in excess growth of fermenting organisms and of methanogens. This contrasts with Schaefer et al. who fed only a limited lactate amount to their culture system and, thus, may have a much smaller fraction of fermentors and methanogens compared to the biofilm in our bioreactor. In the study by Yu et al., unspecified excess hydrogen

**Table 2. Comparison of Kinetic Constants Determined in this Study with Other Studies That Used Batch-Grown Suspended Cultures<sup>a</sup>**

culture	TCE	TCE	<i>cis</i> -DCE	<i>cis</i> -DCE	VC	VC
	$K_m$	$R_{max}$	$K_m$	$R_{max}$	$K_m$	$R_{max}$
SDC-9, grown in gas-phase anaerobic biotrickling filter (this study)	5.3	0.023	6.9	0.005	4.1	0.012
SDC-9, batch grown (Schaefer et al., 2009) <sup>16</sup>	3.2	139.4	2	49.9	14	145.8
PM, batch grown (Yu et al., 2005) <sup>15</sup>	2.8	5.2	1.9	0.9	602	0.1
EV, batch grown (Yu et al., 2005) <sup>15</sup>	1.8	5.2	1.8	0.6	62.6	0.3
VS, batch grown (Cupples et al., 2004) <sup>14</sup>	ND	ND	3.3	3.1	2.6	ND
Uncharacterized culture, batch grown (Fennell and Gossett, 1998) <sup>12</sup>	0.5	5	0.5	5	290	5
Uncharacterized culture, batch grown (Haston and McCarty, 1999) <sup>13</sup>	1.4	0.1	3.3	0.03	2.6	0.02
Uncharacterized culture, batch grown (Garant and Lynd, 1998) <sup>11</sup>	17.4	651.7	11.9	408.3	38.3	463.2

<sup>a</sup>  $R_{max}$  values are in  $\mu\text{moles mg}_{\text{protein}}^{-1} \text{h}^{-1}$ , and  $K_m$  values are in  $\mu\text{M}$ .

and butanol were added to cultures used for kinetic constants determination, but it is not mentioned whether any methanogenesis was observed.

While all  $K_m$  values for TCE and *cis*-DCE determined in this study are in the same order of magnitude as those determined by others, the values determined here are at the higher end of the spectrum. This could be a result of immobilization of the bacteria on a support, as discussed later. Interestingly, the  $K_m$  values for VC for both the cultures used by Yu et al.<sup>15</sup> are one to two orders of magnitude higher than those determined by us. Higher  $K_m$  values suggest cometabolic transformation as also shown by Fennell and Gossett<sup>12</sup> for VC, and thus, it could be that the PM and EV cultures used by Yu et al. contain reductive dehalogenases responsible for metabolic transformation of only TCE and *cis*-DCE, but not VC. However, the EV culture was later documented to contain both VcrA and BvcA enzymes,<sup>8</sup> responsible for metabolic transformation of VC, and thus, it is unclear why the  $K_m$  value for VC for the EV culture was also significantly higher than those reported for metabolic transformation of VC.<sup>13,14</sup>

**Inhibitions between Various Compounds.** First, experiments were conducted with a mixture of VC and *cis*-DCE, with one concentration of VC and either absence of, or two different concentrations of *cis*-DCE. The kinetic constants for *cis*-DCE were determined considering that there was no inhibition from *cis*-DCE on VC dechlorination. Thus, if the data from these experiments fitted the model well, both the biokinetic constants for *cis*-DCE as well as the hypothesis of no inhibition of *cis*-DCE on VC dechlorination could be validated. Figure 5 shows the comparison of experimental data with model simulations considering no inhibition of *cis*-DCE on VC dechlorination. The model simulations compare well with the experimental data, and thus, it can be concluded that *cis*-DCE indeed did not inhibit the dechlorination of VC.

Next, experiments were performed with *cis*-DCE and TCE together, with one fixed concentration of *cis*-DCE in absence of, or with two different concentrations of TCE. Figure 6 shows a comparison of the experimental data with model simulations considering (a) competitive inhibition of TCE on *cis*-DCE dechlorination and (b) no inhibition of TCE on *cis*-DCE dechlorination. Visual observation of the model predictions for the *cis*-DCE evolution in the presence of TCE (squares and triangles) as well as an analysis of the residuals show that the model that includes competitive inhibition of TCE on *cis*-DCE dechlorination (Figure 6a) describes the observed data better.

The finding that TCE inhibits *cis*-DCE dechlorination, but *cis*-DCE does not inhibit VC dechlorination, suggests that the

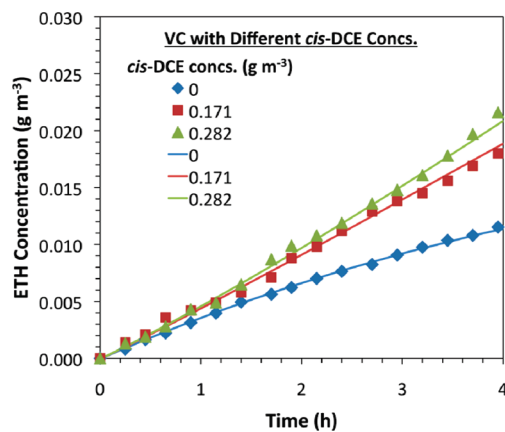


**Figure 5.** Comparison of experimental data (symbols) and model predictions (considering no inhibition of *cis*-DCE on VC, lines) for experiments with VC and *cis*-DCE together. The initial VC concentration was  $0.05 \text{ g m}^{-3}$ . Legend shows initial concentrations of *cis*-DCE in  $\text{g m}^{-3}$ .

reduction of *cis*-DCE was carried out by a single reductive dehalogenase (viz. TceA), while the reduction of VC was carried out by a separate reductive dehalogenase (viz. VcrA). While it is known that *Dehalococcoides ethenogenes* strain 195 that contains the TceA enzyme cannot metabolically dechlorinate VC,<sup>4</sup> strains that contain the VcrA enzyme (viz. strain FL2 and strain VS) are able to dechlorinate *cis*-DCE metabolically.<sup>5,30</sup> However, the transformation rates for *cis*-DCE by protein extracts of VcrA are reported to be at least 1 order of magnitude lower than those by protein extracts of TceA.<sup>31,32</sup> The relative enzyme affinities for *cis*-DCE for VcrA are also reported to be much lower than those for TceA,<sup>30</sup> suggesting that it is likely that the enzymes in our system may not be acting on all compounds together, with various specificities developed for different compounds over the duration of continuous treatment. Holmes et al.<sup>33</sup> also observed a similar specificity of TceA toward *cis*-DCE and of VcrA toward VC for a mixed culture containing the two reductive dehalogenases.

Next, experiments were performed with VC and TCE together, with one concentration of VC and either absence of, or two different concentrations of TCE. Figure 7 shows a comparison of the experimental data with model predictions considering (a) competitive inhibition of TCE on VC dechlorination and (b) no inhibition of TCE on VC dechlorination. It should be stressed that model simulations reported in Figure 7 are predictions, hence that they contain no adjustable parameters. While the model

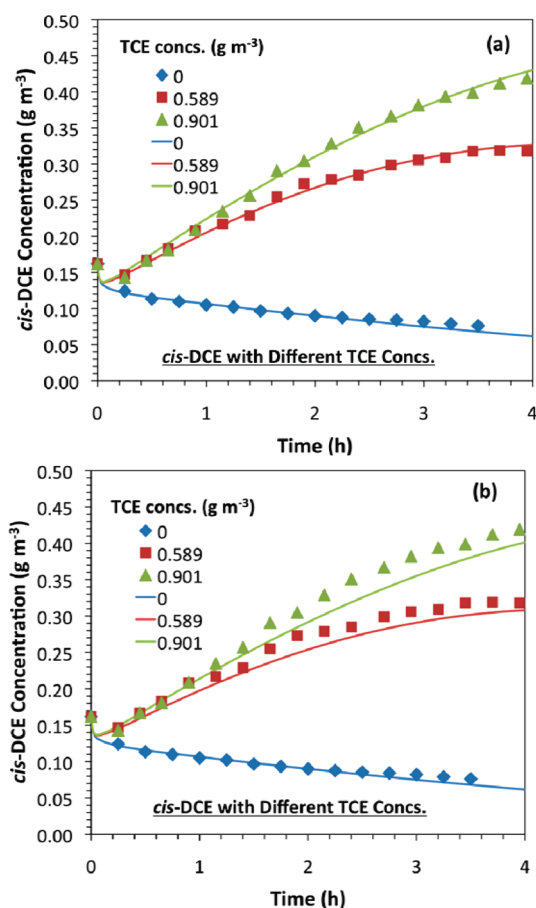


**Figure 6.** Comparison of experimental data (symbols) and model predictions (lines) (a: competitive inhibition of TCE on *cis*-DCE; b: no inhibition) for experiments with *cis*-DCE and TCE together. The initial *cis*-DCE concentration was  $0.162 \text{ g m}^{-3}$ . Legend shows initial concentrations of TCE in  $\text{g m}^{-3}$ .

considering competitive inhibition of TCE on VC dechlorination severely underestimates the rate of ethene generation from VC dechlorination, even the model considering no inhibition does not compare well with the experimental data, as it overestimates ethene concentrations. This result suggests that there is some sort of inhibition of TCE on VC dechlorination. Because VcrA can also dechlorinate TCE, it is unlikely that this inhibition could be noncompetitive. If this inhibition is competitive, the estimated  $K_m$  value for TCE does not describe well the inhibition on VC dechlorination (Figure 7 a). The fact that the  $K_m$  value of TCE required for suitable fit should be much higher than the value reported in Table 1 points to the possibility that VC is converted primarily by VcrA, while TCE by TceA and only to some extent by VcrA. The affinity of TCE for VcrA is much lower than that for the TceA enzyme,<sup>31,32</sup> and thus, the estimated overall  $K_m$  value for TCE, which possibly reflects affinity primarily for the TceA enzyme, does not correlate with the competitive inhibition of TCE on VC. To accurately describe this inhibition, it would be necessary to determine the  $K_I$  value of TCE on VC in a system that contains only the VcrA enzyme.

**Relevance of Present Study.** In this study, the biokinetic constants for reductive dechlorination of TCE and its intermediates and various inhibitions for an immobilized culture containing *Dehalococcoides* spp. were determined (Figure 8). Most previous studies have focused on determining biokinetic constants

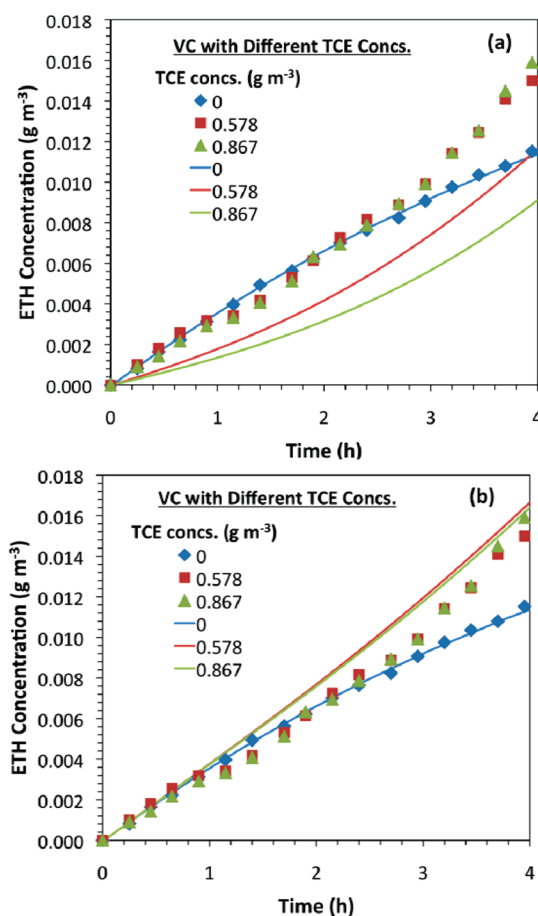


**Figure 7.** Comparison of experimental data (symbols) and model predictions (line) (a: competitive inhibition of TCE on VC, and b: no inhibition) for experiments with VC and TCE together. The initial VC concentration was  $0.05 \text{ g m}^{-3}$ . Legend shows initial concentrations of TCE in  $\text{g m}^{-3}$ .

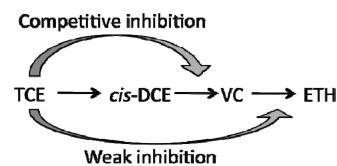


**Figure 8.** Biological inhibitions along the TCE reductive dechlorination pathway as determined in this study.

using suspended cultures; our results indicate that cell immobilization may have an effect on the kinetics. While decrease in specific dechlorination rates can be related to the smaller fraction of *Dehalococcoides* spp. in the biofilm in the current study compared to suspended cultures grown on minimal lactate or hydrogen supply, the decrease in enzyme affinities or increase in  $K_m$  values involves more complex phenomena. Usually, decreases in observed  $K_m$  values for biofilms in comparison to suspended cultures are explained by diffusion limitations within the biofilm;<sup>34</sup> however, in this study, real (by opposition to apparent)  $K_m$  values were determined through curve-fitting of the reaction–diffusion model. Thus, mass transfer limitation effects on  $K_m$  can be excluded. Decreases in actual enzyme affinities in biofilms compared to suspended cultures have been observed before by other researchers,<sup>35</sup> but the reasons for this phenomenon are not well

understood. It is known that physiological changes occur in bacterial cells when grown in a biofilm, and these changes are dependent on the environmental conditions and immobilization surface properties.<sup>36</sup> Also, the genetic regulation of cells grown in a biofilm differs from those that grow in planktonic cultures,<sup>37</sup> especially in response to various stresses or micro-nutrients requirement, thus resulting in changes in measured  $K_m$  values.

It was observed that enzyme affinity for *cis*-DCE was lower than for TCE for *Dehalococcoides* spp. grown in the continuously fed biotrickling filter, and that TCE competitively inhibited dechlorination of *cis*-DCE. Contaminated site and microcosm data from several studies on in situ bioremediation shows that VC generation usually commences only after all TCE is converted to *cis*-DCE or after TCE has reached extremely low concentrations.<sup>10,38–41</sup> This observation is consistent with the finding that when high loads of TCE are applied to the microorganisms, dechlorination of *cis*-DCE is inhibited by TCE. No inhibition of *cis*-DCE on VC dechlorination was observed in this study. While this may not necessarily be true for all sites and cultures, there is the possibility as discussed earlier that both transformations are catalyzed by different reductive dehalogenases. From a literature survey on in situ bioremediation of TCE, it was also found that in most cases ethene production begins even if *cis*-DCE is still not completely dechlorinated to VC, validating that the inhibition of *cis*-DCE on VC dechlorination, if any, is very weak.

A direct implication of competitive inhibitions between various compounds concerns the time required to achieve complete dechlorination in either flow through bioreactors or in situ bioremediation. The presence of TceA and VcrA should eventually result in complete conversion of the various chlorinated ethenes to ethene in a batch-type treatment. The presence of BvcA, which cometabolically converts TCE to *cis*-DCE and metabolically converts *cis*-DCE and VC, along with VcrA during bioremediation, is suggested to result in functional redundancy because both dehalogenases have the same transformation pathways and specificity of electron acceptors. However, for continuous bioreactors, it may be necessary to use a culture containing both these dehalogenases in combination with TceA, so that the transformation of each compound is carried out primarily by a single reductive dehalogenase, resulting in minimal *cis*-DCE and VC accumulation.

## ■ ASSOCIATED CONTENT

**S Supporting Information.** Schematic diagram of the anaerobic biotrickling filter setup for differential operation; comparison of experimental data and model predictions for selected experiments with TCE, *cis*-DCE, and VC (see text for details). This material is available free of charge via the Internet at <http://pubs.acs.org>.

## ■ AUTHOR INFORMATION

### Corresponding Author

\*Phone: (919) 660-5480; fax: (919) 660-5219; e-mail: marc.deshusses@duke.edu.

### Present Addresses

<sup>§</sup>Current address: Center for Environmental Biotechnology, Biodesign Institute, Arizona State University, Tempe, Arizona 85287, United States

## ■ NOMENCLATURE

Z	Biofilm thickness (m)
$C_{G, \text{compd}}$	Concentration of the compound in gas ( $\text{g m}^{-3}$ )
$C_{L, \text{compd}}$	Concentration of the compound in liquid ( $\text{g m}^{-3}$ )
$C_{WB, \text{compd}}$	Concentration of the compound in wetted biofilm ( $\text{g m}^{-3}$ )
$C_{NWB, \text{compd}}$	Concentration of the compound in nonwetted biofilm ( $\text{g m}^{-3}$ )
$C_{SV, \text{compd}}$	Concentration of the compound in sorption volume ( $\text{g m}^{-3}$ )
$C_{GLi, \text{compd}}$	Concentration of the compound at the gas–liquid interface ( $\text{g m}^{-3}$ )
$C_{GBi, \text{compd}}$	Concentration of the compound at the gas–biofilm interface ( $\text{g m}^{-3}$ )
$C_{LBi, \text{compd}}$	Concentration of the compound at the liquid–biofilm interface ( $\text{g m}^{-3}$ )
$D_{e, \text{compd}}$	Effective diffusion coefficient of the compound in the biofilm ( $\text{m}^2 \text{h}^{-1}$ )
$k_G$	Gas film mass transfer coefficient ( $\text{m h}^{-1}$ )
$F_G$	Gas flow rate ( $\text{m}^3 \text{h}^{-1}$ )
$k_L$	Liquid film mass transfer coefficient ( $\text{m h}^{-1}$ )
$F_L$	Liquid flow rate ( $\text{m}^3 \text{h}^{-1}$ )
$R_{\text{max}, \text{compd}}$	Maximum rate of biological reduction of the compound in the biofilm ( $\text{g m}_{\text{biofilm}^{-3}} \text{h}^{-1}$ )
$K_{m, \text{compd}}$	Michaelis–Menten constant for the compound ( $\text{g m}^{-3}$ )
$A_{NW}$	Nonwetted area ( $\text{m}^2$ )
$i$	Number of vertical bed segments (also $N_{\text{bed}}$ )
$j$	Number of horizontal biofilm segments (also $N_{\text{bf}}$ )
$R_{\text{compd}}$	Rate of appearance/disappearance of the compound in the biofilm ( $\text{g m}_{\text{biofilm}^{-3}} \text{h}^{-1}$ )
$V_G$	Volume of gas phase ( $\text{m}^3$ )
$V_L$	Volume of liquid phase ( $\text{m}^3$ )
$V_{SV}$	Volume of sorption volume ( $\text{m}^3$ )
$A_W$	Wetted area ( $\text{m}^2$ )

## ■ REFERENCES

- (1) Petura, J. C. Trichloroethylene and methyl chloroform in groundwater: A problem assessment. *J. Am. Water Works Assoc.* **1981**, *73*, 200–205.
- (2) Moran, M. J.; Zogorski, J. S.; Squillace, P. J. Chlorinated solvents in groundwater of the United States. *Environ. Sci. Technol.* **2007**, *41*, 74–81.
- (3) Papat, S. C.; Deshusses, M. A. Reductive dehalogenation of trichloroethene vapors in an anaerobic biotrickling filter. *Environ. Sci. Technol.* **2009**, *43*, 7856–7861.
- (4) Maymo-Gatell, X.; Chien, Y. T.; Gossett, J. M.; Zinder, S. H. Isolation of a bacterium that reductively dechlorinates tetrachloroethene to ethene. *Science* **1997**, *276*, 1568–1571.
- (5) He, J.; Sung, Y.; Krajmalnik-Brown, R.; Ritalahti, K. M.; Löffler, F. E. Isolation and characterization of *Dehalococcoides* sp. strain FL2, a trichloroethene (TCE)- and 1,2-dichloroethene-respiring anaerobe. *Environ. Microbiol.* **2005**, *7*, 1442–1450.
- (6) Sung, Y.; Ritalahti, K. M.; Apkarian, R. P.; Löffler, F. E. Quantitative PCR confirms purity of strain GT: A novel trichloroethene-to-ethene-respiring *Dehalococcoides* isolate. *Appl. Environ. Microbiol.* **2006**, *72*, 1980–1987.
- (7) Chung, J.; Krajmalnik-Brown, R.; Rittmann, B. E. Bioreduction of trichloroethene using a hydrogen-based membrane biofilm reactor. *Environ. Sci. Technol.* **2008**, *42*, 477–483.
- (8) Azizian, M. F.; Behrens, S.; Sabalowsky, A.; Dolan, M. E.; Spormann, A. M.; Semprini, L. Continuous-flow column study of

reductive dehalogenation of PCE upon bioaugmentation with the Evantite enrichment culture. *J. Contam. Hydrol.* **2008**, *100*, 11–21.

(9) NAVFAC Remediation Innovative Technology Seminar. DCE/VC stall at natural attenuation sites, 2003. <https://portal.navy.mil/portal/page/portal/20055F7546BA51CDE0440003BA8FC471>.

(10) Rahm, B. G.; Chauhan, S.; Holmes, V. F.; Macbeth, T. W.; Sorenson, K. S. J.; Alvarez-Cohen, L. Molecular characterization of microbial populations at two sites with differing reductive dechlorination abilities. *Biodegradation* **2006**, *17*, 523–534.

(11) Garant, H.; Lynd, L. Applicability of competitive and non-competitive kinetics to the reductive dechlorination of chlorinated ethenes. *Biotechnol. Bioeng.* **1998**, *57*, 751–755.

(12) Fennell, D. E.; Gossett, J. M. Modeling the production of and competition for hydrogen in a dechlorinating culture. *Environ. Sci. Technol.* **1998**, *32*, 2450–2460.

(13) Haston, Z. C.; McCarty, P. L. Chlorinated ethene half-velocity coefficients ( $K_s$ ) for reductive dehalogenation. *Environ. Sci. Technol.* **1999**, *33*, 223–226.

(14) Cupples, A. M.; Spormann, A. M.; McCarty, P. L. Vinyl chloride and *cis*-dichloroethene dechlorination kinetics and microorganism growth under substrate limiting conditions. *Environ. Sci. Technol.* **2004**, *38*, 1102–1107.

(15) Yu, S. H.; Dolan, M. E.; Semprini, L. Kinetics and inhibition of reductive dechlorination of chlorinated ethylenes by two different mixed cultures. *Environ. Sci. Technol.* **2005**, *39*, 195–205.

(16) Schaefer, C. E.; Condee, C. W.; Vainberg, S.; Steffan, R. J. Bioaugmentation for chlorinated ethenes using *Dehalococcoides* sp.: Comparison between batch and column experiments. *Chemosphere* **2009**, *75*, 141–148.

(17) Sabalowsky, A. R.; Semprini, L. Trichloroethene and *cis*-1,2-dichloroethene concentration-dependent toxicity model simulates anaerobic dechlorination at high concentrations. II: Continuous flow and attached growth reactors. *Biotechnol. Bioeng.* **2010**, *107*, 540–549.

(18) Sakuma, T.; Hattori, T.; Deshusses, M. A. Comparison of different packing materials for the biofiltration of air toxics. *J. Air Waste Manage. Assoc.* **2006**, *56*, 1567–1575.

(19) Kim, S.; Deshusses, M. A. Development and experimental validation of a conceptual model for biotrickling filter of H<sub>2</sub>S. *Environ. Prog.* **2003**, *22*, 119–128.

(20) Deshusses, M. A.; Hamer, G.; Dunn, I. J. Behavior of biofilters for waste air biotreatment. I. Dynamic-model development. *Environ. Sci. Technol.* **1995**, *29*, 1048–1058.

(21) Gossett, J. M. Measurement of the Henry's law constants of C1 and C2 chlorinated hydrocarbons. *Environ. Sci. Technol.* **1987**, *21*, 202–208.

(22) Chang, P.; Wilke, C. R. Some measurements of diffusion in liquid. *J. Phys. Chem.* **1955**, *59*, 592–596.

(23) Stewart, P. S. A review of experimental measurements of effective diffusive permeabilities and effective diffusion coefficients in biofilms. *Biotechnol. Bioeng.* **1998**, *59*, 261–272.

(24) Ottengraf, S. P. P. Exhaust Gas Purification. In *Biotechnology*; Rhen, H.-J., Reed, G., Eds.; VCH Verlagsgesellschaft: Weinheim, Germany, 1986.

(25) Onda, K.; Takeuchi, H.; Okumoto, Y. Mass transfer coefficients between gas and liquid phases in packed columns. *J. Chem. Eng. Jpn.* **1968**, *1*, 56–62.

(26) Kim, S.; Deshusses, M. A. Determination of mass transfer coefficients for packing materials used in biofilters and biotrickling filters for air pollution control. 2: Development of mass transfer coefficients correlations. *Chem. Eng. Sci.* **2008**, *63*, 856–861.

(27) Cox, H. H. J.; Deshusses, M. A. Biotrickling Filters. In *Bio-reactors for Waste Gas Treatment*; Kennes, C., Veiga, M. C., Eds.; Kluwer Academic Publishers: Dordrecht, The Netherlands, 2001.

(28) Rittmann, B. E.; McCarty, P. L. *Environmental Biotechnology: Principles and Applications*; McGraw-Hill Publishing Co.: New York, 2001.

(29) He, J. Z.; Sung, Y.; Dollhopf, M. E.; Fathepure, B. Z.; Tiedje, J. M.; Löffler, F. E. Acetate versus hydrogen as direct electron donors to

stimulate the microbial reductive dechlorination process at chloroethene-contaminated sites. *Environ. Sci. Technol.* **2002**, *36*, 3945–3952.

(30) Cupples, A. M.; Spormann, A. M.; McCarty, P. L. Growth of a *Dehalococcoides*-like microorganism on vinyl chloride and *cis*-dichloroethene as electron acceptors as determined by competitive PCR. *Appl. Environ. Microbiol.* **2003**, *69*, 953–959.

(31) Magnuson, J. K.; Romine, M. F.; Burris, D. R.; Kingsley, M. T. Trichloroethene reductive dehalogenase from *Dehalococcoides ethenogenes*: Sequence of *tceA* and substrate range characterization. *Appl. Environ. Microbiol.* **2000**, *66*, 5141–5147.

(32) Muller, J. A.; Rosner, B. M.; von Abendroth, G.; Meshulam-Simon, G.; McCarty, P. L.; Spormann, A. M. Molecular identification of the catabolic vinyl chloride reductase from *Dehalococcoides* sp. strain VS and its environmental distribution. *Appl. Environ. Microbiol.* **2004**, *70*, 4880–4888.

(33) Holmes, V. F.; He, J. Z.; Lee, P. K. H.; Alvarez-Cohen, L. Discrimination of multiple *Dehalococcoides* strains in a trichloroethene enrichment by quantification of their reductive dehalogenase genes. *Appl. Environ. Microbiol.* **2006**, *72*, 5877–5883.

(34) Hamdi, M. Biofilm thickness effect on the diffusion limitation in the bioprocess reaction: Biofloc critical diameter significant. *Bioprocess Eng.* **1995**, *12*, 193–197.

(35) Yu, J.; Pinder, K. L. Intrinsic fermentation kinetics of lactose in acidogenic biofilms. *Biotechnol. Bioeng.* **1993**, *41*, 479–488.

(36) Jeffrey, W. H.; Paul, J. H. Activity of an attached and free-living *Vibrio* sp. as measured by thymidine incorporation, p-iodonitrotetrazolium reduction, and ATP/DNA ratios. *Appl. Environ. Microbiol.* **1986**, *51*, 150–156.

(37) Prigent-Combaret, C.; Vidal, O.; Dorel, C.; Lejeune, P. Abiotic surface sensing and biofilm-dependent regulation of gene expression in *Escherichia coli*. *J. Bacteriol.* **1999**, *181*, 5993–6002.

(38) Adamson, D. T.; McDade, J. M.; Hughes, J. B. Inoculation of DNAPL source zone to initiate reductive dechlorination of PCE. *Environ. Sci. Technol.* **2003**, *37*, 2525–2533.

(39) Lendvay, J. M.; Löffler, F. E.; Dollhopf, M.; Aiello, M. R.; Daniels, G.; Fathepure, B. Z.; Gebhard, M.; Heine, R.; Helton, R.; Shi, J.; Krajmalnik-Brown, R.; Major, C. L.; Barcelona, M. J.; Petrovskis, E.; Hickey, R.; Tiedje, J. M.; Adriaens, P. Bioreactive barriers: A comparison of bioaugmentation and biostimulation for chlorinated solvent remediation. *Environ. Sci. Technol.* **2003**, *37*, 1422–1431.

(40) Sleep, B. E.; Seepersad, D. J.; Mo, K.; Heidorn, C. M.; Hrapovic, L.; Morrill, P. L.; McMaster, M. L.; Hood, E. D.; LeBron, C.; Lollar, B. S.; Major, D. W.; Edwards, E. A. Biological enhancement of tetrachloroethene dissolution and associated microbial community changes. *Environ. Sci. Technol.* **2006**, *40*, 3623–3633.

(41) Himmelheber, D. W.; Pennell, K. D.; Hughes, J. B. Natural attenuation processes during in situ capping. *Environ. Sci. Technol.* **2007**, *41*, 5306–5313.

Supporting Information for:

**Kinetics and inhibition of reductive dechlorination of trichloroethene in a continuously-fed anaerobic biofilm reactor**

Sudeep C. Popat, Marc A. Deshusses

*Total pages: 8; Total figures: 8*

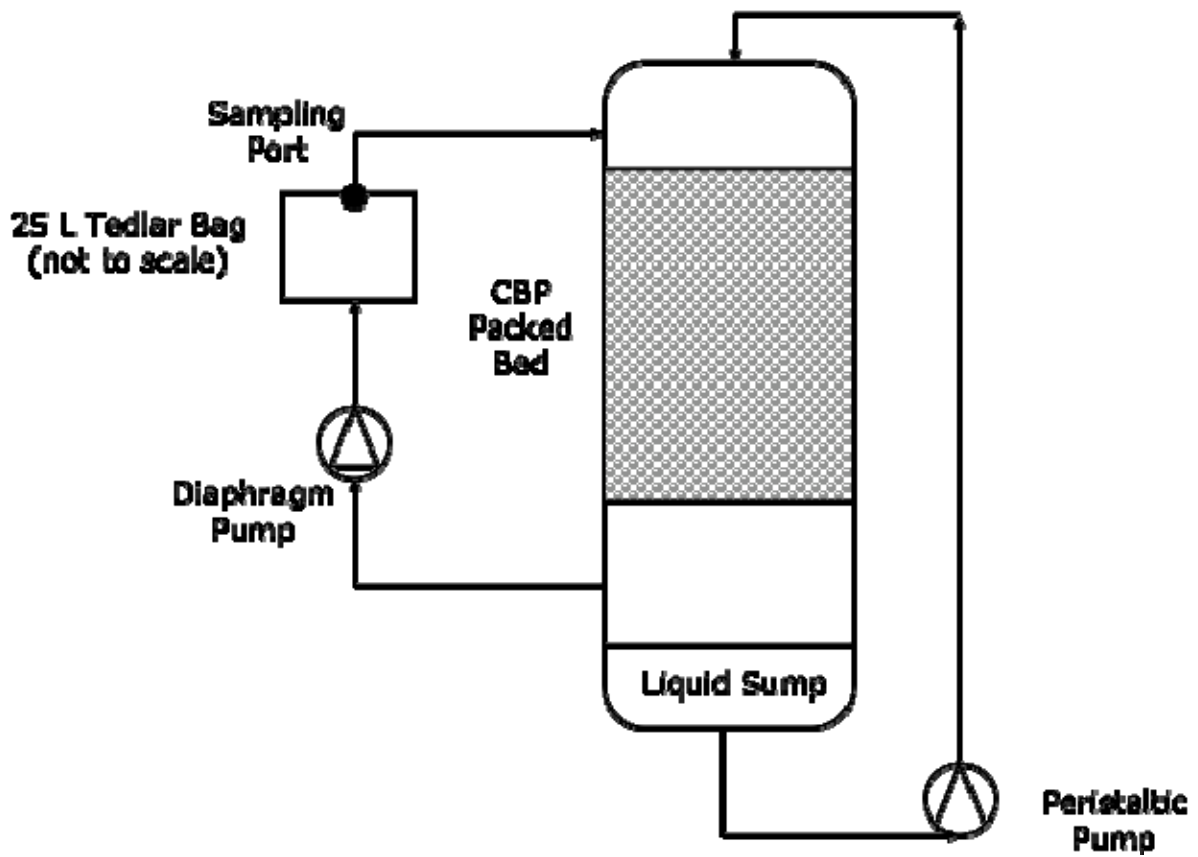


**Figure S1.** Schematic of the biotrickling filter for differential operation (not to scale).

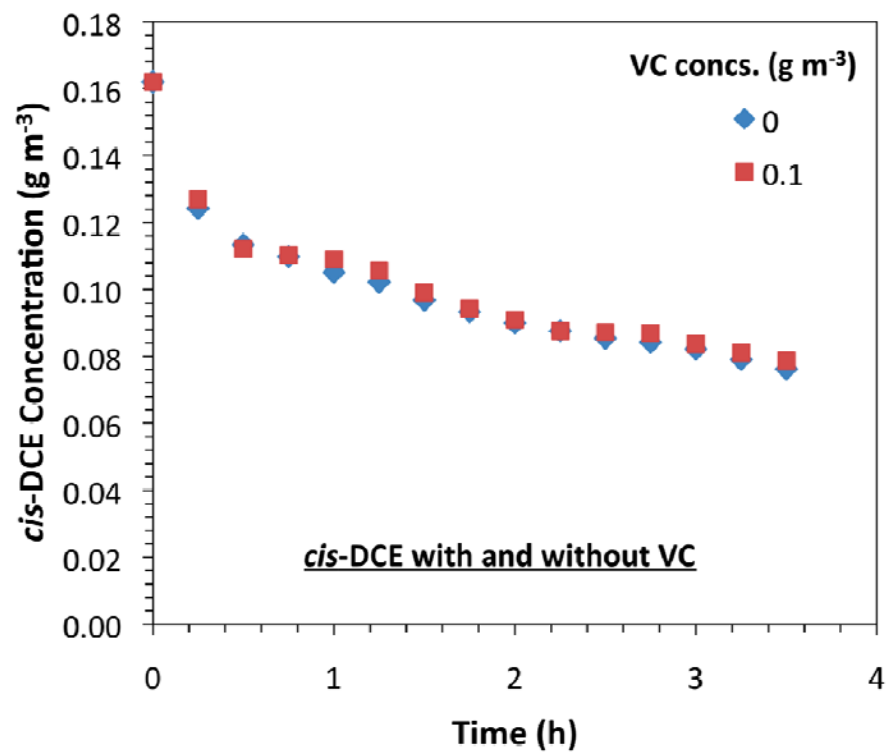


**Figure S2.** Comparison of *cis*-DCE dechlorination in the presence and absence of VC. Legend shows VC concentrations in g m<sup>-3</sup>. The sharp decrease during the first 15 min. is due primarily to absorption of DCE in the trickling liquid.

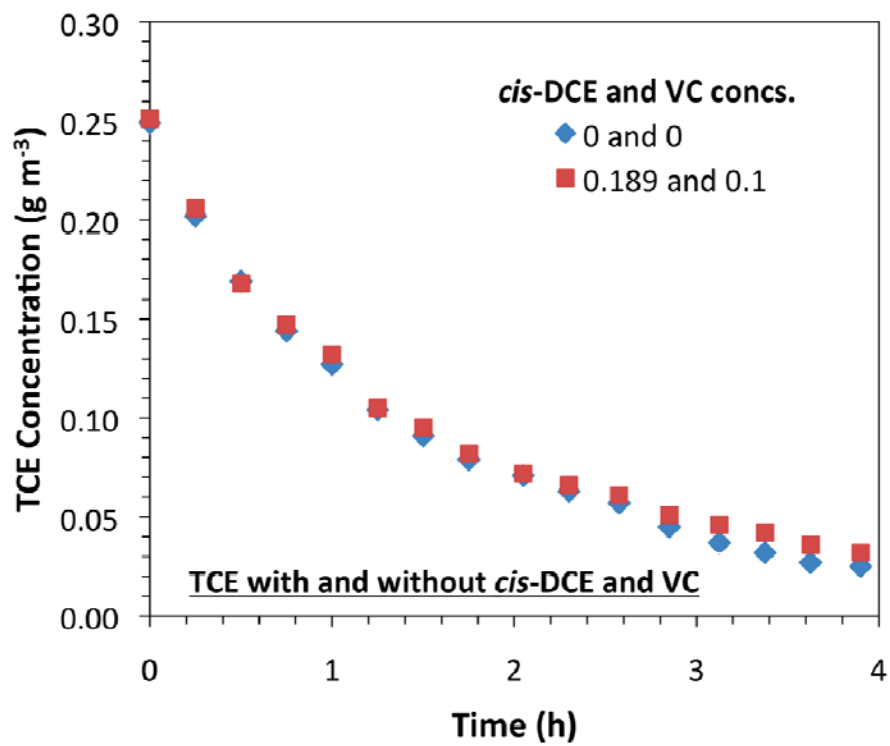


**Figure S3.** Comparison of TCE dechlorination in the presence and absence of *cis*-DCE and VC. Legend shows *cis*-DCE and VC concentrations in g m<sup>-3</sup>.

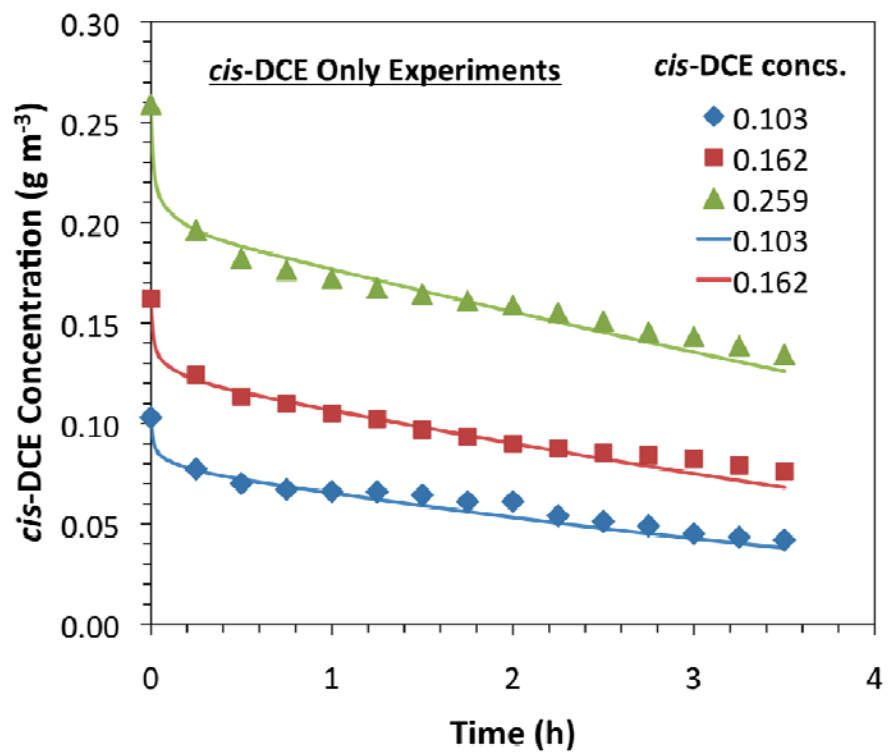


**Figure S4.** Comparison of experimental data (symbols) and model predictions (lines) for *cis*-DCE concentration during *cis*-DCE only experiments. Legend shows initial concentrations of *cis*-DCE in  $\text{g m}^{-3}$ . Model assumes no inhibition from *cis*-DCE on VC dechlorination or vice versa.

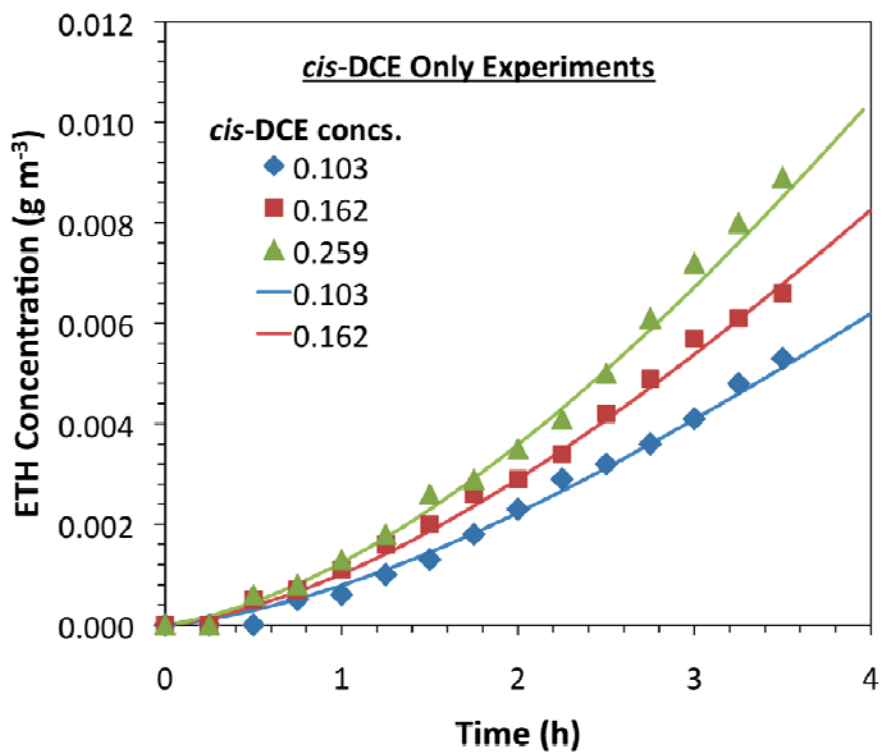


**Figure S5.** Comparison of experimental data (symbols) and model predictions (lines) for ethene concentration during *cis*-DCE only experiments. Legend shows initial concentrations of *cis*-DCE in  $\text{g m}^{-3}$ . Model assumes no inhibition from *cis*-DCE on VC dechlorination or vice versa.

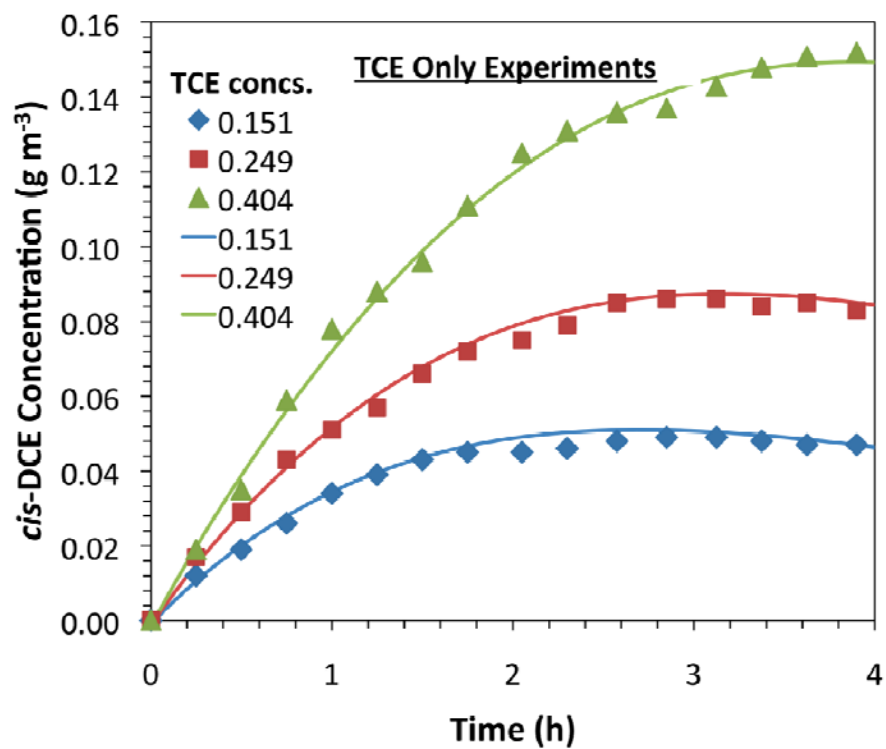


**Figure S6.** Comparison of experimental data (symbols) and model predictions (lines) for *cis*-DCE concentration during TCE-only experiments. Legend shows initial concentrations of TCE in g m<sup>-3</sup>. Model assumes competitive inhibition of TCE on *cis*-DCE dechlorination.

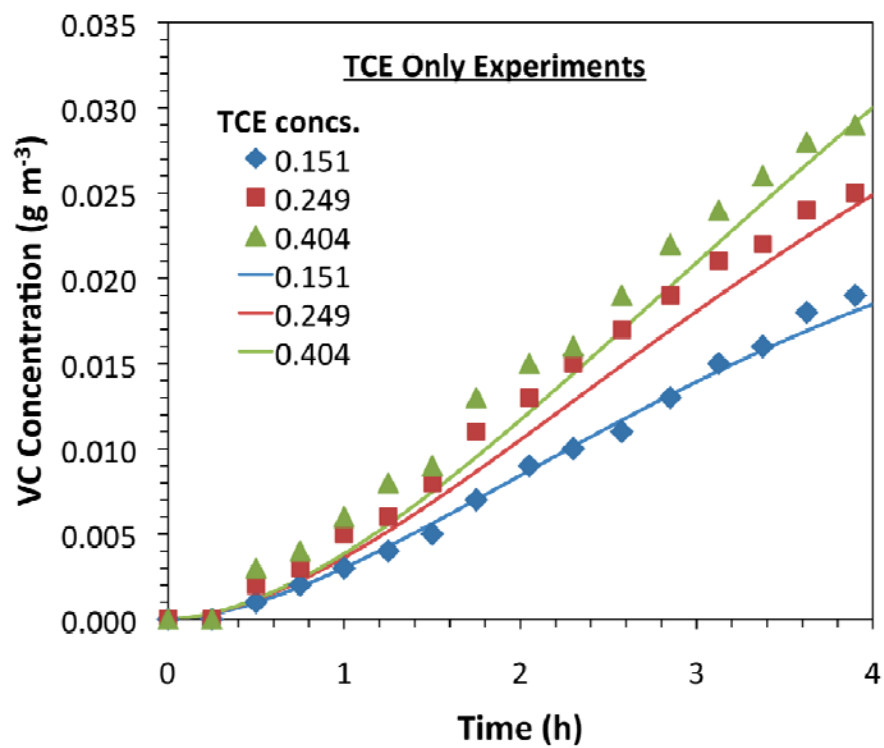


**Figure S7.** Comparison of experimental data (symbols) and model predictions (lines) for VC concentration during TCE-only experiments. Legend shows initial concentrations of TCE in g m<sup>-3</sup>.  
<sup>3</sup>. Model assumes no inhibition of TCE on VC dechlorination.

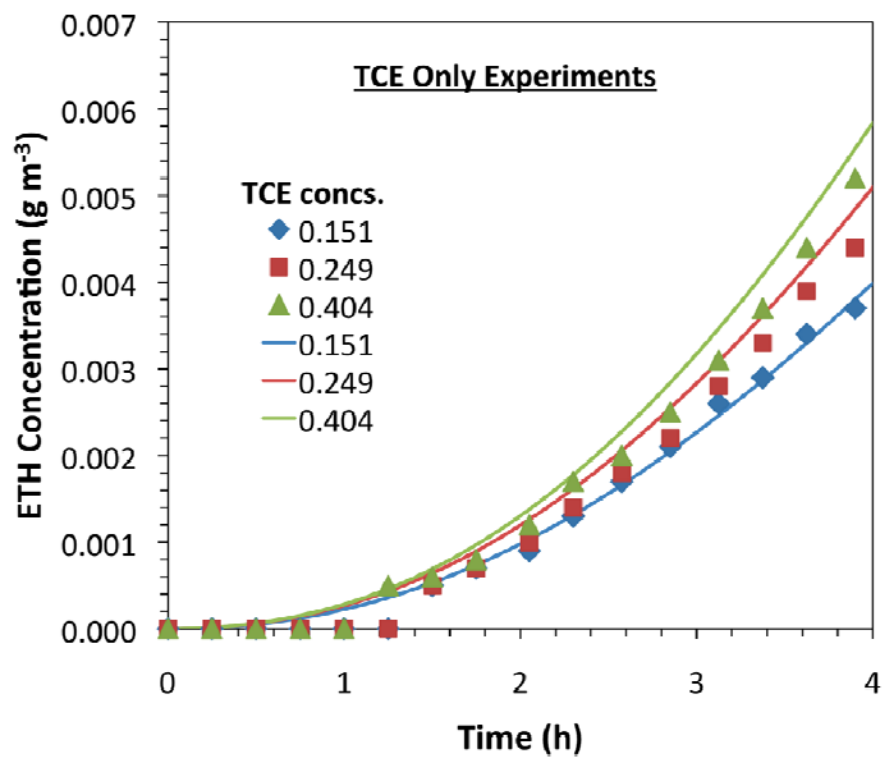


**Figure S8.** Comparison of experimental data (symbols) and model predictions (lines) for ethene concentration during TCE-only experiments. Legend shows initial concentrations of TCE in  $\text{g m}^{-3}$ .<sup>3</sup> Model assumes no inhibition of TCE on VC dechlorination.